MOX–Report No. 31/2009

Theoretical study and numerical simulation of textiles

Paola F. Antonietti, Paolo Biscari,
Alaleh Tavakoli, Marco Verani, Maurizio Vianello

MOX, Dipartimento di Matematica "F. Brioschi"
Politecnico di Milano, Via Bonardi 9 - 20133 Milano (Italy)

mox@mate.polimi.it http://mox.polimi.it

Theoretical study and numerical simulation of textiles

Paola F. Antonietti[♯], Paolo Biscari[♭], Alaleh Tavakoli[♯]
Marco Verani[♯], Maurizio Vianello[♭]

September 26, 2009

[♯] MOX - Laboratorio di Modellistica e Calcolo Scientifico,
Dipartimento di Matematica *Francesco Brioschi*,
Politecnico di Milano
Piazza Leonardo da Vinci 32, 20133 Milano, Italy
paola.antonietti@polimi.it, alaleh.tavakoli@polimi.it,
marco.verani@polimi.it

[♭] Dipartimento di Matematica *Francesco Brioschi*,
Politecnico di Milano,
Piazza Leonardo da Vinci 32,
20133 Milano, Italy
paolo.biscari@polimi.it, maurizio.vianello@polimi.it

Keywords: textile modelling, tricot fabric, anisotropic continua, multi-scale optimization

Abstract

We propose a new approach for developing continuum models fit to describe the mechanical behavior of textiles. We develop a physically motivated model, based on the properties of the yarns, which can predict and simulate the textile behavior. The approach relies on the selection of a suitable topological model for the patch of the textile, coupled with constitutive models for the yarn behavior. The textile structural configuration is related to the deformation through an energy functional, which depends on both the macroscopic deformation and the distribution of internal nodes. We determine the equilibrium positions of these latter, constrained to an assigned macroscopic deformation. As a result, we derive a macroscopic strain energy function, which reflects the possibly nonlinear character of the yarns as well as the anisotropy induced by the microscopic topological pattern. By means of both analytical estimates and numerical experiments, we show that our model is well suited for both academic test cases and real industrial textiles, with particular emphasis on the tricot textile.

1 Introduction

The purpose of this paper is to set up a model fit to investigate the relation between the mechanical properties of the textile and its texture. In order to achieve this objective we develop a multi-scale model for the textile structure, which describes the behavior of the textile under affine deformations.

The mechanical behavior of even relatively simple plain-weave fabric is complex due to the intricate interactions of the yarns forming the fabric mesostructure. Despite the many attempts to develop effective models for fabric behavior, there is currently no widely accepted modeling approach that can accurately capture all the important aspects of fabric deformation and effectively predict both the macroscopic mechanical response of the fabric as well as the response of the component yarns at the mesostructural level. This is due in part to the variability of requirements for fabric models in different applications. Specialized fabric models employing various approaches have been proposed by researchers.

One of the simplest approaches is to homogenize the behavior of the underlying mesostructure and to approximate the fabric as an anisotropic continuum. In the framework of a continuum formulation, a woven fabric can be treated as an anisotropic planar continuum with two preferred material directions. Homogenized formulations for fabrics or fabric composite structures have been proposed by a number of different researchers. In [1, 5] elastoplastic anisotropic continuum formulations for filamentary networks are proposed. In [5, 6, 7] the authors introduce a multiscale model for a fabric material. The model is based on the assumption that on the macroscale the fabric behaves as a continuum membrane, while on the microscale the properties of the microstructure are taken into account by a constitutive law derived by modeling a pair of overlapping crimped yarns as extensible elasticae. Several further efforts deal with the tensile properties of textile fabrics [9, 10, 11, 12]. In the above papers the authors compute the biaxial tensile properties of the plain tricot starting from the structure of the fabric and using some of the mechanical properties of the yarn. A constitutive model for the mechanical behavior of textile fabrics has been proposed in [3], where a new approach for developing continuum models for the mechanical behavior of textile fabrics in planar deformation is proposed. Moreover, in [3] a continuum model that can both simulate existing fabrics and predict the behavior of novel fabrics based on the properties of the yarns and the weave is considered.

In this paper, we present a new model for the mathematical and numerical simulation of the structural properties of textiles. The model of the yarns interaction is derived from the equilibrium response of crossed yarns in contact. This model is then used to derive the energy functional for the textile. The energy functional depends on two types of variables. On the one hand, the macroscopic deformation gradient provides the shape of the textile in the deformed configuration. On the other hand, the internal nodes provide further degrees of freedom, which aim at minimizing the elastic energy of the joining yarns.

The effective energy functional of the macroscopic textile is obtained by minimizing the internal degrees of freedom, that is, by assuming that the internal nodes are immediately able to adjust to the new microscopic panorama induced by the macroscopic deformations. In this minimization process the topology of the texture plays a crucial role: in order to bring the texture properties into light, we introduce and compute a *texture tensor*, which determines the elastic response of the textile. The eigenvalues of such a tensor are the key ingredients in the model we develop: their assessment allows to obtain a quantitative measure of the isotropic or anisotropic character of the textile, and they further provide a measure of the rigidity of the textile response, as a function of the macroscopic deformation.

The constitutive law which governs the yarn elastic response determines the possibly nonlinear character of the textile. We first consider a linear constitutive equation for the yarns. In this particular case, we show that the texture tensor is constant, in the sense that it only depends on the texture topology, and not on the deformation. Then, in order to deal with more realistic cases, we also take into account nonlinear constitutive equations for the yarns, and in this is case, the macroscopic properties of the textile become strain-dependent.

A major point in the model we propose deals with the determination of the position of the internal nodes that minimize the energy functional. To this end we apply the Nelder-Mead algorithm [4, 8], a classical numerical direct search method for multidimensional unconstrained minimization. The numerical results for academic textiles patterns ascertain the accuracy of the method. We next apply our algorithm to more realistic cases, in particular to the tricot textile. The results we obtain confirm that the model is well suited for practical applications.

The outline of the paper is as follows. In Section 2 we present our model and discuss the properties of the energy minimizers. The numerical algorithm is discussed in Section 3; in Section 4 we present the results of a number of numerical experiments, which aim both at validating and using our model. Finally, in Section 5 we draw some conclusions and discuss further research perspectives.

2 Mathematical Model

The approach to textile modeling proposed here is based on a point of view which is both continuum and discrete, since we define an elastic energy associated to a deformation of a given patch of textile through minimization of the total strain energy associated with the (rectilinear) pieces of yarns which crisscross the given patch.

In this section we introduce the appropriate terminology and describe the conceptual framework of our approach. A piece of textile with shape $\mathcal{P}_0$ (such as a square or a rectangle) is given in a reference configuration. However, we do not look at the material as continuous but, rather, as formed by a discrete network of one-dimensional segments of two (possibly different) types of yarns,

which are under tension and obey an elastic constitutive equation, to be specified later on. Each yarn crosses the region $\mathcal{P}_0$ changing direction at points which we identify as knots, where different types of yarns are tied together. A sort of "no slip" condition holds at each knot, so that a piece of straight yarn connecting two adjacent knots is composed always of the same material elements (in other words: we assume infinite friction at knots).

A homogeneous deformation with gradient $\mathbf{F}$ may be assigned to a given subset R of knots, which we think of as being on the boundary of the given patch. Let $\mathcal{P} = \mathbf{F}\mathcal{P}_0$. The deformation described by $\mathbf{F}$ prescribes the displacement of the knots in this set R, while the final position of the remaining knots in the patch $\mathcal{P}$ is computed through minimization of the total strain energy associated to the pieces of yarns connecting adjacent knots. The topology of the piece of fabric under scrutiny is taken into consideration at this level. In other words, in this analysis a relevant goal is the deduction of the macroscopic (*i.e.*, continuous) properties from the description of one-dimensional pieces of yarn.

We now introduce some necessary terminology and notation. First of all we only discuss fabric which is composed by two possibly different types of yarns, denoted as I and II or sometimes as red and blue (the situation in which more than two types of yarns are present would be described by a straighforward extension). Of course, we shall assume that yarns I and II might have different mechanical properties but we take them to be homogeneous along their whole length. We think of each piece of yarn which crosses the given patch of textile as "coming in" from a given knot and "going out" from another knot. Thus, each segment of yarn I or II connecting directly two knots has an orientation.

We denote the position of knots which are present in the reference configuration of patch $\mathcal{P}_0$ by $\boldsymbol{p}$ and index them as $\boldsymbol{p}_i$, with $i \in \mathcal{N} := \{1, 2, 3, \ldots, N\}$. Next, we say that knot $\boldsymbol{p}_i$ is directly I-connected (resp. II-connected) to knot $\boldsymbol{p}_j$ if there is a piece of yarn I (resp. II) which goes from $\boldsymbol{p}_i$ to $\boldsymbol{p}_j$. A visualization of a patch of textile we have in mind is shown in Figure 1. It also evidences a common property in textile patches, that is, the presence of a basic cell whose replication allows to cover the complete region $\mathcal{P}_0$.

For later use it is useful to create two sets of pair of indexes $(i, j) \in \mathcal{N} \times \mathcal{N}$. We let C_{I} (resp. C_{II}) be the set of pairs $(i, j) \in \mathcal{N} \times \mathcal{N}$ such that: (1) $i \neq j$; (2) $\boldsymbol{p}_i$ is directly I-connected to $\boldsymbol{p}_j$ (resp. II-connected). We list as many copies of a given pair (i, j) in C_{I} as there are yarns of type I directly connecting $\boldsymbol{p}_i$ to $\boldsymbol{p}_j$, and we do the same for C_{II}.

Without loss of generality we consider homegeneous deformations which leave the origin fixed and are described by $\mathbf{x} = \mathbf{F}\mathbf{p}$, where $\mathbf{F}$ is a tensor with positive determinant and Cartesian components

$$\mathbf{F} = \begin{bmatrix} a & b \\ c & d \end{bmatrix}.$$

The coordinates of the position vectors of points $\mathbf{p}$ and $\mathbf{x}$ are given by $\mathbf{p} = [X, Y]$,

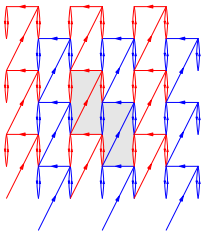

Figure 1: An example of reference configuration $\mathcal{P}_0$. The basic periodicity cell is evidenced in gray.

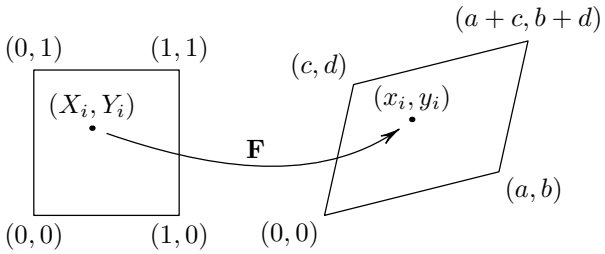

Figure 2: A homogeneous finite deformation.

$\mathbf{x} = [x, y]$, so that we may write

$$\begin{cases} x = aX + bY, \\ y = cX + dY, \end{cases}$$

a deformation which we visualize in Figure 2.

The subset of knots $\mathbf{p}$ on which $\mathbf{F}$ acts is written as R and its typical element as $\mathbf{r}$. We think of points $\mathbf{r}$ as being held fixed by some sort of external device after the deformation $\mathbf{F}$ is applied, which is then viewed as a constraint. The remaining set of knots, which we collectively denote through the letter $\mathbf{q}$, are then free to move and to adjust their position in order to minimize a strain energy which is associated to yarns I and II. For better clarity we write $\mathbf{y}$ for the present position of points $\mathbf{r} \in R$ (whose position in space is determined by $\mathbf{F}$), and we write $\mathbf{w}$ for the present position of points $\mathbf{q}$, which are free to move around.

Each piece of yarn I and II directly connecting two adjacent knots has a strain energy which we take to be a prescribed function of the distance between them. More precisely,

$$U_{\mathrm{I}}(|\mathbf{x}_i - \mathbf{x}_j|), \quad (i,j) \in C_{\mathrm{I}}, \qquad U_{\mathrm{II}}(|\mathbf{x}_i - \mathbf{x}_j|), \quad (i,j) \in C_{\mathrm{II}}.$$

where functions U_{I} and U_{II} may be different, since they may describe yarns with different material properties.

The total strain energy is computed as

$$U(\mathbf{x}) := \sum_{(i,j)\in C_{\mathrm{I}}} U_{\mathrm{I}}(|\mathbf{x}_i - \mathbf{x}_j|) + \sum_{(i,j)\in C_{\mathrm{II}}} U_{\mathrm{II}}(|\mathbf{x}_i - \mathbf{x}_j|). \tag{1}$$

Notice that the totality of points $\mathbf{x}$ is formed by two different subsets: points $\mathbf{y}$ whose position is prescribed by $\mathbf{F}$, and are thus not free to move, and points $\mathbf{w}$ which try to get to a position which minimizes the total strain energy. It is therefore sometimes convenient to think of $U(\mathbf{x})$ as a function $U(\mathbf{w}, \mathbf{y})$ of two sets of variables, where $\mathbf{y} = \mathbf{Fr}$. (For the sake of simplicity we omit indexes when a whole set of points is taken into consideration.)

The elastic strain energy for patch $\mathcal{P}_0$ associated with the deformation $\mathbf{F}$ is defined as

$$E(\mathbf{F}) = \min_{\mathbf{w}} U(\mathbf{w}, \mathbf{Fr}). \tag{2}$$

The density of elastic energy (per unit of surface) is obtained from $E(\mathbf{F})$ through a division by $A(\mathcal{P}_0)$, the area of the given patch $\mathcal{P}_0$ in the reference configuration, and is thus defined as

$$W(\mathbf{F}) := E(\mathbf{F})/A(\mathcal{P}_0). \tag{3}$$

We have thus reached the key point of our model. The fabric under discussion is viewed as an elastic (two-dimensional) continuum, where the stored energy for a given strain tensor $\mathbf{F}$ is computed from the mechanical constitutive equations for yarns I and II, which are knitted together according to some topological rules and, at a smaller scale, make up the essential and real structure of the textile to be modelled. In this paper we present some numerical experiments with yarn strain energies U_{I} and U_{II} both linear and nonlinear, which are meant to check that relevant results can be derived.

2.1 Linear yarns

First of all we investigate linearly elastic yarns, for which we choose

$$\begin{aligned} U_{\mathrm{I}}(\mathbf{x}_i, \mathbf{x}_j) &= \frac{1}{2} K_{\mathrm{I}} |\mathbf{x}_i - \mathbf{x}_j|^2, \quad (i,j) \in C_{\mathrm{I}}, \\ U_{\mathrm{II}}(\mathbf{x}_i, \mathbf{x}_j) &= \frac{1}{2} K_{\mathrm{II}} |\mathbf{x}_i - \mathbf{x}_j|^2, \quad (i,j) \in C_{\mathrm{II}}, \end{aligned} \tag{4}$$

where K_{I} and K_{II} are the elastic constants of yarns I and II. Each straight piece of the yarns, connecting two adjacent knots, is thus viewed as a simple linearly elastic spring.

After the introduction of Cartesian coordinates of points $\mathbf{x}_i = (x_i, y_i)$ the total strain energy $U(\mathbf{x})$ can be written as

$$\begin{aligned} U(\mathbf{x}) &= \sum_{(i,j)\in C_{\mathrm{I}}} \frac{1}{2} K_{\mathrm{I}} (\mathbf{x}_i - \mathbf{x}_j)^2 + \sum_{(i,j)\in C_{\mathrm{II}}} \frac{1}{2} K_{\mathrm{II}} (\mathbf{x}_i - \mathbf{x}_j)^2 \\ &= \sum_{(i,j)\in C_{\mathrm{I}}} \frac{1}{2} K_{\mathrm{I}} \big((x_i - x_j)^2 + (y_i - y_j)^2\big) + \sum_{(i,j)\in C_{\mathrm{II}}} \frac{1}{2} K_{\mathrm{II}} \big((x_i - x_j)^2 + (y_i - y_j)^2\big). \end{aligned}$$

The following Proposition shows that, in the linear case, it is possible to carry out the minimization process which provides the equilibrium positions $\mathbf{w}$ of the free knots when the restricted nodes are transformed through $\mathbf{F}$.

Proposition 2.1 *Let $\{\mathbf{p}_i\}$ denote the equilibrium positions of the knots in the reference configuration (*i.e.*, when $\mathbf{F} = \mathbf{I}$). Then, the equilibrium configuration when $\mathbf{F}$ acts on the restricted knots is simply obtained by transforming through $\mathbf{F}$ the reference equilibrium positions. In other words, the minimum of $U(\mathbf{w}, \mathbf{Fr})$ is attained when $\mathbf{w} = \mathbf{Fp}$.*

Let further $\mathbf{C} := \mathbf{F}^T\mathbf{F}$ be the (symmetric and positive definite) right Cauchy-Green strain tensor [2], and $\mathbf{\Lambda}$ be the (symmetric and positive semi-definite) texture tensor, *defined as*

$$\mathbf{\Lambda}(\mathbf{p}) := \sum_{(i,j)\in C_{\mathrm{I}}} K_{\mathrm{I}}(\mathbf{p}_i - \mathbf{p}_j) \otimes (\mathbf{p}_i - \mathbf{p}_j) + \sum_{(i,j)\in C_{\mathrm{II}}} K_{\mathrm{II}}(\mathbf{p}_i - \mathbf{p}_j) \otimes (\mathbf{p}_i - \mathbf{p}_j), \quad (5)$$

where $\otimes$ denotes the standard tensor product. Then,

$$E(\mathbf{C}) = \frac{1}{2}\mathbf{C} \cdot \mathbf{\Lambda} \qquad \textit{and} \qquad \bar{\mathbf{S}} = \mathbf{\Lambda}/A(\mathcal{P}_0), \quad (6)$$

where $\bar{\mathbf{S}}$ is the second *Piola-Kirchhoff stress tensor, defined in terms of $\mathbf{S}$ and $\mathbf{T}$ (the* first *Piola-Kirchhoff and the Cauchy stress tensor, respectively) as [2]*

$$\bar{\mathbf{S}} = \mathbf{F}^{-1}\mathbf{S} = (\det \mathbf{F})\mathbf{F}^{-1}\mathbf{T}\mathbf{F}^{-T}. \quad (7)$$

Proof. The position of points $\mathbf{q}$ which minimizes the total energy $U(\mathbf{p}) = U(\mathbf{q}, \mathbf{r})$ in the reference configuration is such that the resultant force acting on each point is null. In the linear model this force can be written as

$$\mathbf{f}(\mathbf{q}_i) = \sum_{j\in C_{\mathrm{I}}(i)} K_{\mathrm{I}}(\mathbf{p}_j - \mathbf{q}_i) + \sum_{j\in C_{\mathrm{II}}(i)} K_{\mathrm{II}}(\mathbf{p}_j - \mathbf{q}_i),$$

where $C_{\mathrm{I}}(i)$ is the collection of all j such that (i, j) or (j, i) belongs to C_{I} (a similar definition holds for $C_{\mathrm{II}}(i)$). Then, obviously, if we apply $\mathbf{F}$ to all points we obtain

$$\mathbf{f}(\mathbf{F}\mathbf{q}_i) = \sum_{j\in C_{\mathrm{I}}(i)} K_{\mathrm{I}}(\mathbf{F}\mathbf{p}_j - \mathbf{F}\mathbf{q}_i) + \sum_{j\in C_{\mathrm{II}}(i)} K_{\mathrm{II}}(\mathbf{F}\mathbf{p}_j - \mathbf{F}\mathbf{q}_i),$$

and, in view of linearity,

$$\mathbf{f}(\mathbf{F}\mathbf{q}_i) = \sum_{j\in C_{\mathrm{I}}(i)} K_{\mathrm{I}}\mathbf{F}(\mathbf{p}_j - \mathbf{q}_i) + \sum_{j\in C_{\mathrm{II}}(i)} K_{\mathrm{II}}\mathbf{F}(\mathbf{p}_j - \mathbf{q}_i) = \mathbf{F}\mathbf{f}(\mathbf{q}_i).$$

In particular, if the total force acting on node $\mathbf{q}_i$ is zero for $\mathbf{F} = \mathbf{I}$, then it also vanishes in a configuration obtained applying $\mathbf{F}$ to all points, which proves our first assertion.

Moreover, if we let $\mathbf{x} = \mathbf{F}\mathbf{p}$, we deduce that $U(\mathbf{x}) = U(\mathbf{F}\mathbf{p})$ can be written as

$$\begin{aligned}
2U(\mathbf{x}) &= \sum_{(i,j)\in C_{\mathrm{I}}} K_{\mathrm{I}}(\mathbf{x}_i - \mathbf{x}_j)^2 + \sum_{(i,j)\in C_{\mathrm{II}}} K_{\mathrm{II}}(\mathbf{x}_i - \mathbf{x}_j)^2 \\
&= \sum_{(i,j)\in C_{\mathrm{I}}} K_{\mathrm{I}}(\mathbf{F}\mathbf{p}_i - \mathbf{F}\mathbf{p}_j)\cdot(\mathbf{F}\mathbf{p}_i - \mathbf{F}\mathbf{p}_j) \\
&\qquad\qquad + \sum_{(i,j)\in C_{\mathrm{II}}} K_{\mathrm{II}}(\mathbf{F}\mathbf{p}_i - \mathbf{F}\mathbf{p}_j)\cdot(\mathbf{F}\mathbf{p}_i - \mathbf{F}\mathbf{p}_j) \\
&= \sum_{(i,j)\in C_{\mathrm{I}}} K_{\mathrm{I}}\mathbf{F}(\mathbf{p}_i - \mathbf{p}_j)\cdot\mathbf{F}(\mathbf{p}_i - \mathbf{p}_j) + \sum_{(i,j)\in C_{\mathrm{II}}} K_{\mathrm{II}}\mathbf{F}(\mathbf{p}_i - \mathbf{p}_j)\cdot\mathbf{F}(\mathbf{p}_i - \mathbf{p}_j) \\
&= \sum_{(i,j)\in C_{\mathrm{I}}} K_{\mathrm{I}}\mathbf{F}^T\mathbf{F}(\mathbf{p}_i - \mathbf{p}_j)\cdot(\mathbf{p}_i - \mathbf{p}_j) + \sum_{(i,j)\in C_{\mathrm{II}}} K_{\mathrm{II}}\mathbf{F}^T\mathbf{F}(\mathbf{p}_i - \mathbf{p}_j)\cdot(\mathbf{p}_i - \mathbf{p}_j).
\end{aligned}$$

In view of the identity $\mathbf{C}\mathbf{a}\cdot\mathbf{b} = \mathbf{C}\cdot\mathbf{a}\otimes\mathbf{b}$, the expression for $U(\mathbf{x})$ can be written as

$$\begin{aligned}
2U(\mathbf{x}) &= \sum_{(i,j)\in C_{\mathrm{I}}} K_{\mathrm{I}}\mathbf{C}(\mathbf{p}_i - \mathbf{p}_j)\cdot(\mathbf{p}_i - \mathbf{p}_j) + \sum_{(i,j)\in C_{\mathrm{II}}} K_{\mathrm{II}}\mathbf{C}(\mathbf{p}_i - \mathbf{p}_j)\cdot(\mathbf{p}_i - \mathbf{p}_j) \\
&= \mathbf{C}\cdot\left[\sum_{(i,j)\in C_{\mathrm{I}}} K_{\mathrm{I}}(\mathbf{p}_i - \mathbf{p}_j)\otimes(\mathbf{p}_i - \mathbf{p}_j) + \sum_{(i,j)\in C_{\mathrm{II}}} K_{\mathrm{II}}(\mathbf{p}_i - \mathbf{p}_j)\otimes(\mathbf{p}_i - \mathbf{p}_j)\right].
\end{aligned}$$

If we now define the texture tensor $\mathbf{\Lambda}$ as in (5), the energy corresponding to the equilibrium configuration for a prescribed $\mathbf{F}$ can be computed as $U(\mathbf{x}) = \frac{1}{2}\mathbf{C}\cdot\mathbf{\Lambda}(\mathbf{p})$. When points $\mathbf{q}$ (which are free to move) are in the equilibrium configuration $\mathbf{q}^*$, while points $\mathbf{r}$ are fixed by some external constraint, we have $E(\mathbf{C}) = \frac{1}{2}\mathbf{C}\cdot\mathbf{\Lambda}(\mathbf{p})$. (We remark that, because of frame-indifference, it is to be expected that the strain energy is a function of the strain tensor $\mathbf{C}$, rather than of $\mathbf{F}$ alone.)

The strain energy per unit surface W determines the second Piola-Kirchhoff stress tensor $\bar{\mathbf{S}}$ through [2]

$$\bar{\mathbf{S}} = 2\frac{\partial W}{\partial \mathbf{C}}. \tag{8}$$

From $W(\mathbf{C}) = E(\mathbf{C})/A(\mathcal{P}_0) = \frac{1}{2}\mathbf{C}\cdot\mathbf{\Lambda}(\mathbf{p})/A(\mathcal{P}_0)$, we compute

$$\frac{\partial W}{\partial \mathbf{C}} = \frac{1}{2}\,\mathbf{\Lambda}/A(\mathcal{P}_0).$$

In view of (8), we conclude that $\bar{\mathbf{S}} = \mathbf{\Lambda}/A(\mathcal{P}_0)$, which completes the proof. □

We remark that, in this linear case, the texture tensor can be derived by determining the equilibrium positions of the knots $\mathbf{q}$ in the reference configuration. Thus, the detailed knowledge of the equilibrium reference configuration allows to determine the strain energy and the stress tensors for any other configuration

obtained through $\mathbf{F}$. In particular, for $\mathbf{m}$ the unit normal pointing outwards from a region, the vector $\mathbf{F}\bar{\mathbf{S}}\mathbf{m} = \mathbf{\Lambda}\mathbf{m}/A(\mathcal{P}_0)$ is the force per unit length acting on the boundary, as measured in the reference configuration.

Equation (6) shows that the second Piola-Kirchhoff stress tensor is proportional to the texture tensor. In particular, it is constant, in the sense that it does not depend on the strain. Nevertheless, this does by no means imply that the traction necessary to obtain a prescribed deformation does not depend on the strain itself. Indeed, if we invert equation (7), and then make use of (6), we can prove that

$$\mathbf{T}(\mathbf{F}) = \frac{1}{A(\mathcal{P})}\,\mathbf{F}\mathbf{\Lambda}\mathbf{F}^T, \quad \text{since} \quad A(\mathcal{P}) = A(\mathcal{P}_0)\det\mathbf{F}.$$

We note that a homothety does not affect the stress tensor, since the deformation gradient is simply multiplied by the dilation factor, and the area scales as the square of the dilation factor itself. This fact is a consequence of the absence of any intrinsic length in the definition of the quadratic potential (4).

We can give a precise meaning to the components of tensor $\mathbf{\Lambda}$ as normal and shear stresses. Moreover, notice that the material symmetry of the strain energy $W(\mathbf{C})$ can be computed from the action of the rotation group on $\mathbf{\Lambda}$. Indeed, for a rotation $\mathbf{Q}$ of the reference configuration we have that $\mathbf{F} \mapsto \mathbf{F}^* := \mathbf{F}\mathbf{Q}$ and, as a consequence, $\mathbf{C} \mapsto \mathbf{C}^* := \mathbf{Q}^T\mathbf{C}\mathbf{Q}$. Thus, $W(\mathbf{C}^*) = \mathbf{Q}^T\mathbf{C}\mathbf{Q}\cdot\mathbf{\Lambda} = \mathbf{C}\cdot\mathbf{Q}\mathbf{\Lambda}\mathbf{Q}^T$ and $W(\mathbf{C}^*) = W(\mathbf{C})$, for all $\mathbf{F}$, if and only if

$$\mathbf{\Lambda} = \mathbf{Q}\mathbf{\Lambda}\mathbf{Q}^T. \tag{9}$$

In conclusion, the symmetry group of $W(\mathbf{C})$ is the set of all rotations $\mathbf{Q}$ such that (9) holds.

Remark 2.1 *A symmetric tensor $\mathbf{\Lambda}$ on a two dimensional vector space has only two possibilities:*

(a) the eigenvalues are equal, and so $\mathbf{\Lambda}$ is a multiple of the identity and the material is isotropic, since (9) *is satisfied by any rotation $\mathbf{Q}$;*

(b) the eigenvalues are different and the material is orthotropic respect to the material directions corresponding to the orthogonal eigenvectors of $\mathbf{\Lambda}$.

We identify the Cartesian components of the symmetric tensor $\mathbf{\Lambda}$ through

$$\mathbf{\Lambda} = \begin{bmatrix} \lambda_{11} & \lambda_{12} \\ \lambda_{21} & \lambda_{22} \end{bmatrix} \tag{10}$$

and, in view of definition (5), we easily compute them as

$$\lambda_{11} = \sum_{(i,j)\in C_{\rm I}} K_{\rm I}\big(X_i - X_j\big)^2 + \sum_{(i,j)\in C_{\rm II}} K_{\rm II}\big(X_i - X_j\big)^2,$$

$$\lambda_{12} = \lambda_{21} = \sum_{(i,j)\in C_{\rm I}} K_{\rm I}\big(X_i - X_j\big)\,(Y_i - Y_j) + \sum_{(i,j)\in C_{\rm II}} K_{\rm II}\,(X_i - X_j)\,(Y_i - Y_j)\,,$$

$$\lambda_{22} = \sum_{(i,j)\in C_{\rm I}} K_{\rm I}\big(Y_i - Y_j\big)^2 + \sum_{(i,j)\in C_{\rm II}} K_{\rm II}\big(Y_i - Y_j\big)^2.$$

where $\mathbf{p}_i = (X_i, Y_i)$.

Remark 2.2 *The eigenvalues $\lambda_{\max}$ and $\lambda_{\min}$ of $\mathbf{\Lambda}$ are useful for describing the elastic properties of the patch of fabric under exam, since they essentially coincide with the principal stresses. We can easily and explicitly compute the maximum and minimum eigenvalue as the real roots of the characteristic equation of $\mathbf{\Lambda}$. The eigenvectors then correspond to the direction of principal stresses of the tensor $\bar{\mathbf{S}}$.*

2.2 Nonlinear yarns

We now move a step forward, and take into account nonlinear generalizations of the yarn energy. The equilibrium energy per unit surface W, as defined in (2) and (3), is now to be computed through a minimization process over the possible positions $\mathbf{w}_i$ of the unconstrained knots, for any fixed value of the deformation $\mathbf{F}$ acting on the knots $\mathbf{r}_j$, once a choice of the topological structure of the yarn connections among knots has been made. The situation is now significantly more complex than in the linear case and numerical experiments become necessary to obtain both qualitative and quantitative information on any given fabric.

In the following we will show how we can extract from the results of the numerical simulations the mechanical properties of the possibly nonlinear and anisotropic materials. First, we show how suitable derivatives of the density of elastic energy help us in reconstructing the second Piola-Kirchhoff stress tensor $\bar{\mathbf{S}}$. Next, we derive from it the Cauchy stress tensor $\mathbf{T}$, which eventually determines how the elastic response of the textile depends on the imposed deformation.

Let $\mathbf{F}_0$ represent a finite deformation with respect to the reference configuration. For any given tensor $\mathbf{U}$, we define the one-parameter family of deformations $\mathbf{F}_{\mathbf{U}}(t) = \mathbf{F}_0 + t\mathbf{U}$, with $t \in [0, \bar{t}]$. When $\bar{t}$ is sufficiently small, $\det \mathbf{F}_{\mathbf{U}}(t) \neq 0$, and thus $\mathbf{F}_{\mathbf{U}}(t)$ represents another admissible deformation. We denote by $W_{\mathbf{U}}(t)$ the density of elastic energy obtained by optimizing the position of the internal nodes when the deformation $\mathbf{F}_{\mathbf{U}}(t)$ is applied on the constrained knots. The following proposition relates the second Piola-Kirchhoff stress tensor to $W_{\mathbf{U}}(t)$.

Proposition 2.2 *Let $W_{\mathbf{U}}(t)$ be defined as above in terms of the deformation $\mathbf{F}_{\mathbf{U}}(t)$. Let further $\bar{\mathbf{S}}$ be the second Piola-Kirchhoff stress tensor associated with*

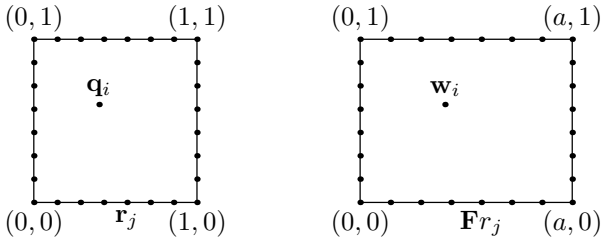

Figure 3: A family of pure stretches parametrized by a.

the deformation $\mathbf{F}_0$*. Then*

$$\dot{W}_{\mathbf{U}}(0) = \bar{\mathbf{S}} \cdot \mathrm{sym}(\mathbf{F}_0^T \mathbf{U}), \tag{11}$$

where a dot denotes differentiation with respect to the parameter t*.*

Proof. Let $\mathbf{F}_{\mathbf{U}}(t) = \mathbf{F}_0 + t\mathbf{U}$. Then $\mathbf{C}_{\mathbf{U}}(t) = \mathbf{F}_{\mathbf{U}}^T(t)\mathbf{F}_{\mathbf{U}}(t)$, so that

$$\dot{\mathbf{C}}_{\mathbf{U}}(0) = \mathbf{F}_0^T \mathbf{U} + \mathbf{U}^T \mathbf{F}_0 = 2\,\mathrm{sym}(\mathbf{F}_0^T \mathbf{U}).$$

Then, by using (8) we obtain

$$\dot{W}_{\mathbf{U}}(0) = \frac{\partial W_{\mathbf{U}}}{\partial \mathbf{C}} \cdot \dot{\mathbf{C}}_{\mathbf{U}}(0) = \bar{\mathbf{S}}(\mathbf{F}_0) \cdot \mathrm{sym}(\mathbf{F}_0^T \mathbf{U}). \qquad \square$$

The repeated application of equation (11), with suitable choices of the tensor $\mathbf{U}$, allows to arrive at the complete expression of $\bar{\mathbf{S}}$:

$$\begin{aligned}
\mathbf{U}_1 &= \mathbf{F}_0^{-T}\big(\mathbf{e}_x \otimes \mathbf{e}_x\big) \quad &\Rightarrow \quad \bar{S}_{11} &= \dot{W}_{\mathbf{U}_1}(0) \\
\mathbf{U}_2 &= \mathbf{F}_0^{-T}\big(\mathbf{e}_x \otimes \mathbf{e}_y\big) \quad &\Rightarrow \quad \bar{S}_{12} &= \dot{W}_{\mathbf{U}_2}(0) = S_{21} \\
\mathbf{U}_3 &= \mathbf{F}_0^{-T}\big(\mathbf{e}_y \otimes \mathbf{e}_y\big) \quad &\Rightarrow \quad \bar{S}_{22} &= \dot{W}_{\mathbf{U}_3}(0),
\end{aligned} \tag{12}$$

where $\{\mathbf{e}_x, \mathbf{e}_y\}$ are the unit vectors of the Cartesian basis. Once $\bar{\mathbf{S}}$ has been obtained, the Cauchy stress tensor may be obtained from (7)

$$\mathbf{T} = \frac{1}{\det \mathbf{F}_0}\, \mathbf{F}_0\, \bar{\mathbf{S}}\, \mathbf{F}_0^T. \tag{13}$$

To better illustrate the above procedure, we now explicitly consider the case in which $\mathbf{F}_0$ is a uniaxial extension, which represents the most common experiment, both in numerical simulations and in real applications. We consider a square patch and apply a pure stretch in the direction of the x axis

$$\mathbf{F}_0 = a\,\mathbf{e}_x \otimes \mathbf{e}_x + \mathbf{e}_y \otimes \mathbf{e}_y\,. \tag{14}$$

We remind that $\mathbf{F}_0$ is to be interpreted as a constraint on the position of the boundary knots when determining the equilibrium configuration of the set of free

knots $\mathbf{w}_i$, according to the topological structure of the textile patch. In Figure 3 the dots on the boundary correspond to points whose position is constrained by the homogeneous deformation $\mathbf{F}_0$, while $\mathbf{q}_i$ and $\mathbf{w}_i$ describe points which, in the present configuration, adjust their position in order to minimize the energy U. From (12) and (14) we obtain

$$\mathbf{U}_1 = a^{-1}\,\mathbf{e}_x \otimes \mathbf{e}_x, \qquad \mathbf{U}_2 = a^{-1}\,\mathbf{e}_x \otimes \mathbf{e}_y, \qquad \mathbf{U}_3 = \mathbf{e}_y \otimes \mathbf{e}_y.$$

Once the above tensors have been used to compute $\dot{W}_{\mathbf{U}_i}(0)$, equations (12) and (13) provide

$$\begin{aligned} \bar{\mathbf{S}} = \;& \dot{W}_{\mathbf{U}_1}(0)\,\mathbf{e}_x \otimes \mathbf{e}_x + \dot{W}_{\mathbf{U}_2}(0)\big(\mathbf{e}_x \otimes \mathbf{e}_y + \mathbf{e}_y \otimes \mathbf{e}_x\big) + \qquad \dot{W}_{\mathbf{U}_3}(0)\,\mathbf{e}_y \otimes \mathbf{e}_y \\ \mathbf{T} = \;& a\dot{W}_{\mathbf{U}_1}(0)\,\mathbf{e}_x \otimes \mathbf{e}_x + \dot{W}_{\mathbf{U}_2}(0)\big(\mathbf{e}_x \otimes \mathbf{e}_y + \mathbf{e}_y \otimes \mathbf{e}_x\big) + a^{-1}\dot{W}_{\mathbf{U}_3}(0)\,\mathbf{e}_y \otimes \mathbf{e}_y. \end{aligned} \tag{15}$$

The Cauchy stress tensor completely characterizes the mechanical properties of the textile after the deformation $\mathbf{F}_0$. We will, in particular, trace the behaviour of the *principal stresses*, that is the eigenvalues of $\mathbf{T}$. Their average will evidence the hardening character of the typical nonlinear responses, while their relative difference will be a measure of the anisotropy of the material.

3 Numerical Discretization

In this section we discuss the issue of the numerical approximation of the following problem: find the position of internal nodes such that the energy functional (1) is minimized. Such a problem is an unconstrained optimization problem, and in order to efficiently solve it we make use of the Nelder-Mead algorithm which is an iterative method for minimizing a real-valued function $f(\mathbf{x})$, $\mathbf{x} \in \mathbb{R}^n$, that is, find $\mathbf{x}^* \in \mathbb{R}^n$ such that $f(\mathbf{x}^*) \leq f(\mathbf{x})$ for all $\mathbf{x} \in I(\mathbf{x}^*)$, with $I(\mathbf{x}^*)$ a suitable neighborhood of $\mathbf{x}^*$.

We describe the algorithm in the bi-dimensional case we are addressing, i.e., $n = 2$.

Given an initial guess, at the k-th iteration, we assume that the points $\mathbf{x}_j^{(k)} \in \mathbb{R}^2$, $j = 1, 2, 3$ that are the vertices of a non-degenerate simplex Δ_k are available, then the Nelder-Mead algorithm computes the vertices $\mathbf{x}_{j+1}^{(k)}$, $j = 1, 2, 3$, as follows.

Algorithm 3.1

1. Order the three vertices $\mathbf{x}_1^{(k)}$, $\mathbf{x}_2^{(k)}$, $\mathbf{x}_3^{(k)}$ to satisfy

$$f(\mathbf{x}_1^{(k)}) \leq f(\mathbf{x}_2^{(k)}) \leq f(\mathbf{x}_3^{(k)}).$$

2. Let $\mathbf{x}_b^{(k)} := (\mathbf{x}_1^{(k)} + \mathbf{x}_2^{(k)} + \mathbf{x}_3^{(k)})/3$ be the barycenter of the triangle identified by $\mathbf{x}_1^{(k)}$, $\mathbf{x}_2^{(k)}$ and $\mathbf{x}_3^{(k)}$. If $\mathbf{x}_b^{(k)}$ and $\mathbf{x}^*$ are sufficiently

close (in a suitable sense) we set $\mathbf{x}^* = \mathbf{x}_c^{(k)}$ and the algorithm ends, otherwise we go to step 3.

3. Compute the reflection point $\mathbf{x}_r^{(k)} = 2\bar{\mathbf{x}}^{(k)} - \mathbf{x}_3^{(k)}$, where $\bar{\mathbf{x}}^{(k)} = (\mathbf{x}_1^{(k)} + \mathbf{x}_2^{(k)})/2$ is the centroid of the best two points.

   (a) If $f(\mathbf{x}_1^{(k)}) \le f(\mathbf{x}_r^{(k)}) \le f(\mathbf{x}_2^{(k)})$, we set

   $$\mathbf{x}_1^{(k+1)} = \mathbf{x}_1^{(k)}, \qquad \mathbf{x}_2^{(k+1)} = \mathbf{x}_2^{(k)}, \qquad \mathbf{x}_3^{(k+1)} = \mathbf{x}_r^{(k)},$$

   and we begin a new iteration step.

   (b) If $f(\mathbf{x}_r^{(k)}) \le f(\mathbf{x}_1^{(k)})$, the reflection step has produced a new minimizer (that means that $\mathbf{x}^*$ could lie outside Δ_k). Therefore, we compute the expansion point $\mathbf{x}_e^{(k)} = 2\mathbf{x}_r^{(k)} - \bar{\mathbf{x}}^{(k)}$.

   (b.1) If $f(\mathbf{x}_e^{(k)}) < f(\mathbf{x}_1^{(k)})$, we set

   $$\mathbf{x}_1^{(k+1)} = \mathbf{x}_1^{(k)}, \qquad \mathbf{x}_2^{(k+1)} = \mathbf{x}_2^{(k)}, \qquad \mathbf{x}_3^{(k+1)} = \mathbf{x}_e^{(k)},$$

   and we begin a new iteration step.

   (b.2) If $f(\mathbf{x}_e^{(k)}) > f(\mathbf{x}_1^{(k)})$, since $f(\mathbf{x}_r^{(k)}) < f(\mathbf{x}_1^{(k)})$, we set

   $$\mathbf{x}_1^{(k+1)} = \mathbf{x}_1^{(k)}, \qquad \mathbf{x}_2^{(k+1)} = \mathbf{x}_2^{(k)}, \qquad \mathbf{x}_3^{(k+1)} = \mathbf{x}_r^{(k)},$$

   and we begin a new iteration step.

4. If $f(\mathbf{x}_r^{(k)}) > f(\mathbf{x}_2^{(k)})$, then the minimizer probably lies within a subset of Δ_k. We therefore generate a contraction point $\mathbf{x}_c^{(k)}$ as

$$\mathbf{x}_c^{(k)} = \begin{cases} \frac{1}{2}(\mathbf{x}_r^{(k)} + \bar{\mathbf{x}}^{(k)}) & \text{if } f(\mathbf{x}_r^{(k)}) < f(\mathbf{x}_3^{(k)}), \\ \frac{1}{2}(\mathbf{x}_3^{(k)} + \bar{\mathbf{x}}^{(k)}) & \text{otherwise.} \end{cases}$$

   (a) If $f(\mathbf{x}_c^{(k)}) < f(\mathbf{x}_3^{(k)})$ and $f(\mathbf{x}_c^{(k)}) < f(\mathbf{x}_r^{(k)})$, we set

   $$\mathbf{x}_1^{(k+1)} = \mathbf{x}_1^{(k)}, \qquad \mathbf{x}_2^{(k+1)} = \mathbf{x}_2^{(k)}, \qquad \mathbf{x}_3^{(k+1)} = \mathbf{x}_c^{(k)},$$

   and we begin a new iteration step.

   (b) If $f(\mathbf{x}_c^{(k)}) \ge f(\mathbf{x}_3^{(k)})$ or if $f(\mathbf{x}_c^{(k)}) \ge f(\mathbf{x}_r^{(k)})$, then n new points are generated.

Figure 4 (top) shows the Nelder-Mead simpleces after reflection and an extension step, Figure 4 (bottom) shows the Nelder-Mead simpleces after an (outside) contraction.

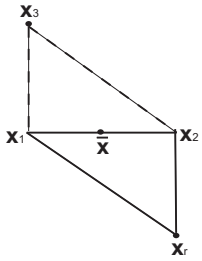

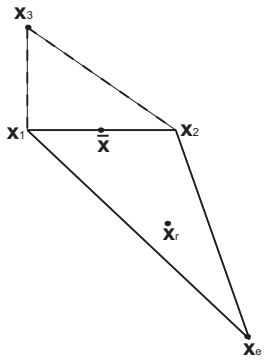

(a) Nelder-Mead simpleces after a reflexion (left) and an extension (right) step.

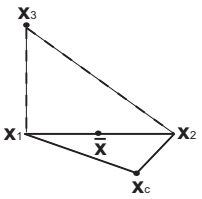

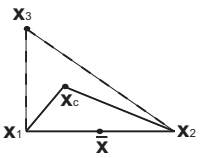

(b) Nelder-Mead simpleces after an outside contraction (left) and a contraction (right) step.

Figure 4: Sample of Nelder-Mead algorithm steps. The original simplex is shown with a dashed line.

4 Numerical Experiments

In this section we present the result of some numerical experiments which test the capabilities of our model. The results we present have been obtained with *MATLAB*®. We address the question of estimating the elastic properties of some textiles with a given texture, by considering both linear/academic and nonlinear/realistic industrial test cases. The strain energy is defined as in equation (1), with a potential U to be specified below. In our experiments we restrict attention to *planar* textiles. Thus, we assume that a reference plane π exists, such that all the node positions lie in π both in the reference and in the actual configuration. Tests have been performed on square grids of 10×10 nodes in the reference configuration. Among the 100 resulting nodes, 36 lie on the boundary, and are thus constrained by the macroscopic deformation. The positions of the remaining 64 internal nodes are thus determined through the optimization algorithm described in Section 3.

4.1 Linear yarns

We have first considered a linear model, based upon the potential given in (4). Two topological patterns are considered below, each of which is allowed to be weaved with two different yarns. To ease the presentation in the linear case, we identify yarn I with the red color, and yarn II with the blue color, and write $K_{\text{red}} \equiv K_{\text{I}}$, $K_{\text{blue}} \equiv K_{\text{II}}$.

Textile-90

The pattern we identify as *Textile-90* is assumed to consist of two families of continuously distributed yarns which, in the reference configuration shown in Figure 5, are orthogonal to each other when crossing. Each *blue* yarn is knitted alternatively with two *red* yarns, which respectively lie on its left and its right. To better explain Figure 5, we remark that the knots (which represent the nodes whose position is to be optimized) are evidenced as blue squares, while at the crossings in which no square is illustrated no interaction between the crossing yarns occurs. The two sets of yarns have allowed to possess different material properties, represented by different values of their elastic constants.

Since an overall multiplying constant may clearly be factorized out from the elastic energy, we fix the value of $K_{\text{red}} = 1$, and analyze how the equilibrium configurations and material properties depend on the value of the ratio $K_{\text{blue}}/K_{\text{red}}$. Figure 6 shows the results obtained for different values of K_{blue}. We have computed the eigenvalues $\lambda_{\max} \geq \lambda_{\min}$ of the texture tensor $\mathbf{\Lambda}$ (see (5) and (10)). The material properties are then expressed in the last two columns through the average strength $\bar{\lambda} = \frac{1}{2}(\lambda_{\max} + \lambda_{\min})$ and the anisotropy $\Delta = (\lambda_{\max} - \lambda_{\min})/\lambda_{\max} \in [0, 1]$. Isotropic textures ($\Delta = 0$, or $\lambda_{\min} = \lambda_{\max}$) are obtained if and only if the elastic constants coincide, and the anisotropy increases monotonically with the ratio $K_{\text{blue}}/K_{\text{red}}$.

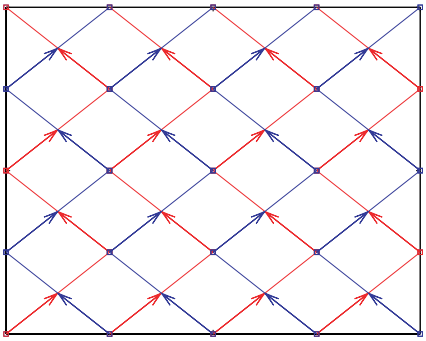

Figure 5: Reference configuration for the Textile-90 pattern.

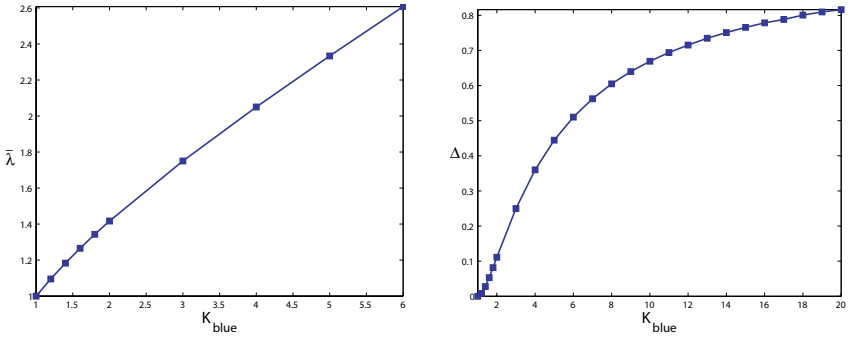

(a) Average eigenvalue $\bar{\lambda}$ (b) Anisotropy Δ

Figure 6: Elastic properties of the Textile-90 pattern as a function of K_{blue}. (The elastic constant K_{red} has been set equal to unity.)

As we already pointed out in Remark 2.1 and Remark 2.2, $\lambda_{\max}$ and $\lambda_{\min}$ essentially coincide with the principal stresses of the textile. Whenever $\Delta > 0$, the material is orthotropic with respect to the directions identified by the corresponding eigenvectors, which yield the principal material directions.

Figure 7 illustrates how the equilibrium configuration of the internal nodes depends on the ratio $K_{\text{blue}}/K_{\text{red}}$. As K_{blue} increases, the increasing rigidity of the blue yarns manifests in the shortening of the blue paths, which thus tend to align parallel. Their orientation does clearly coincide with the direction of the eigenvector associated with the maximum eigenvalue $\lambda_{\max}$, which consequently diverges as K_{blue} increases. On the contrary $\lambda_{\min}$ remains bounded, since its corresponding eigendirection is orthogonal to the blue yarns, and $K_{\text{red}} = 1$. As a consequence, complete anisotropy ($\Delta \to 1$, or $\lambda_{\min}/\lambda_{\max} \to 0$) is approached in the $K_{\text{blue}} \gg K_{\text{red}}$ limit. This is an important feature, since it shows that in this topology it is not sufficient to harden the elastic properties of one of the two yarns in order to harden the whole material.

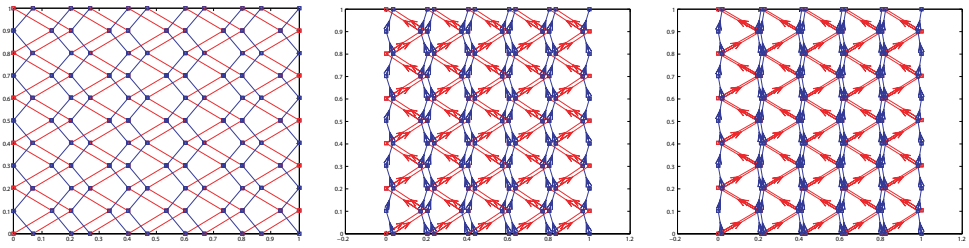

(a) $K_{\text{blue}} = 2$ (b) $K_{\text{blue}} = 5$ (c) $K_{\text{blue}} = 10$

Figure 7: Equilibrium configurations for Textile-90 pattern when $K_{\text{red}} = 1$.

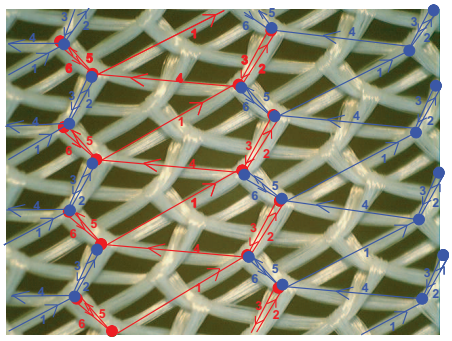

Figure 8: Textile tricot: reference configuration. (Courtesy of Carvico s.p.a.)

Tricot

Our second texture models the tricot fabric. In a tricot, the yarns follow a complex topological pattern, illustrated in Figure 8. We have run in this case the same set of experiments as before. Figure 9 illustrates the results of the same numerical experiments reported in Figure 6. While the average rigidity $\bar{\lambda}$ does confirm its monotonic, almost-linear behavior, the complex topological pattern completely modifies the behavior of the anisotropy Δ. In particular, it is not possible to obtain an isotropic ($\Delta = 0$) textile for any value of K_{blue}. Moreover, the minimum value of Δ is not attained when $K_{\text{blue}} = K_{\text{red}}$, but rather when $K_{\text{blue}}/K_{\text{red}} \approx 2.87$.

The equilibrium configurations for choices $K_{\text{blue}} = K_{\text{red}}$ and $K_{\text{blue}} = 5K_{\text{red}}$ are shown in Figure 10. The left panel is to be compared with the reference textile configuration shown in Figure 8. The overlap between the the two pictures is satisfactory, as the presence of a similar periodicity pattern reveals. The right panel evidences that, as K_{blue} increases, the textile approaches the same type of equilibrium configuration we have already encountered in the Textile-90 case. The stronger blue yarns minimize their path by align almost parallel to the y-direction, which becomes the principal direction associated with $\lambda_{\max}$. Meanwhile, the weaker red yarns perform much longer paths, mostly parallel to the x-direction, which in turn becomes the principal direction associated with

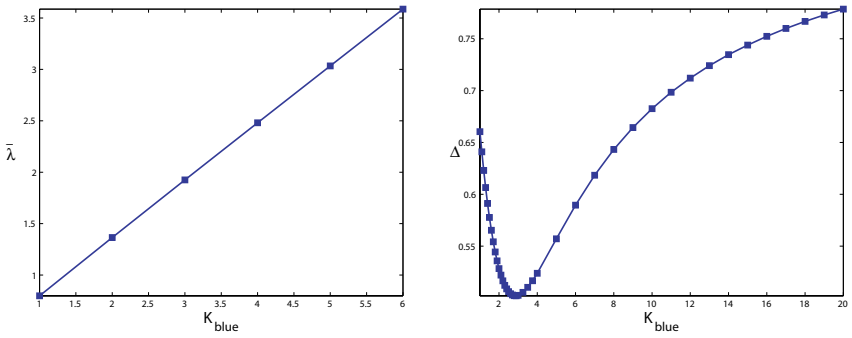

(a) Average eigenvalue $\bar{\lambda}$ (b) Anisotropy Δ

Figure 9: Elastic properties of the tricot pattern as a function of K_{blue}. (The elastic constant K_{red} has been set equal to unity.)

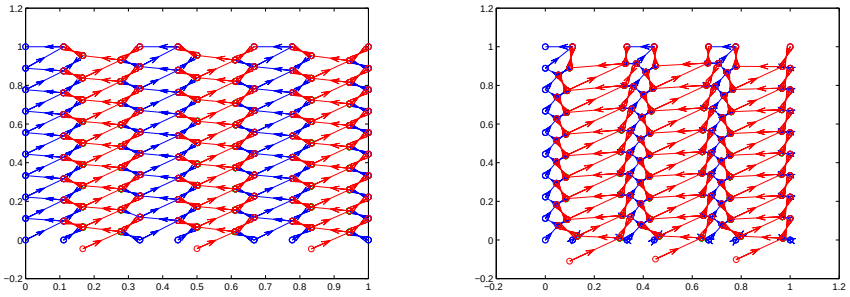

(a) $K_{\text{blue}} = 1$ (b) $K_{\text{blue}} = 5$

Figure 10: Equilibrium configurations for the tricot pattern when $K_{\text{red}} = 1$.

$\lambda_{\min}$. This is the microscopic reason why $\lambda_{\min}$ remains bounded whatever the value of K_{blue} is, so that again $\Delta \to 1$ as $K_{\text{blue}}/K_{\text{red}} \to \infty$. In particular, we find that even in this complex topology it does not suffice to harden one of the two involved elastic constants in order to retrieve a hard textile in all directions.

4.2 Nonlinear tricot textile

In this section we restrict attention to the tricot topology, and consider a nonlinear model for the yarns. In order to simulate the properties of a standard tricot fabric, as the one shown in Figure 8, we moreover assume that the elastic properties of red and blue yarns are identical. All the yarns will thus obey to the same nonlinear constitutive equation, which will replace Eq. (4). The nonlinear potential we adopt is given by $U(\mathbf{x}_i, \mathbf{x}_j) = U_{\text{NL}}(|\mathbf{x}_i - \mathbf{x}_j|)$, with

$$U_{\text{NL}}(d) = \frac{1}{2}K_1 d^2 + \frac{1}{2}K_2\, H(d - d_1)\left((d - d_1)^2 + \frac{(d - d_1)^4}{d_2^2}\right), \qquad (16)$$

where H is the Heaviside step function, K_1, K_2 are elastic constants, and d_1, d_2 are characteristic lengths we will discuss below.

The microscopic model underlying equation (16) is the following. We consider a textile in which each yarn is in fact composed by two different types of threads. The first is an elastomer, which is an extremely flexible material which preserves a linear response up to remarkable strains. Its response is thus represented by the term proportional to K_1 in (16). The second type of thread is of polymeric origin, and it is initially knitted in excess. This means that, as long as the distance between two adjacent knots does not exceed a tunable threshold (modelled by d_1 in (16)), the second thread is not in tension and it does not contribute to the energy minimization. When, on the contrary, the distance d exceeds d_1, the second thread comes on stage. The length d_2 is a characteristic length which identifies the length at which the nonlinear character of the polymer shows off. The physically relevant case is $d_2 \lesssim d_1$, since typically the polymeric material induces a nonlinear response as soon as the initial threshold is exceeded. When coming to numerical simulations, we have set K_1 equal to unity, since again an overall multiplying factor does not qualitatively influence the results. In the results reported below, we have fixed $K_2 = 5$, $d_1 = 0.1$, and $d_2 = 0.15$.

In the linear case, investigated in the previous section, the second Piola-Kirchhoff stress tensor does not depend on the deformation itself. Thus, the texture tensor contains all the relevant information about the mechanical response of the textile. When, on the contrary, nonlinear yarns are considered, we need to make resort to equation (15) to compute the stress tensors $\bar{\mathbf{S}}$ and $\mathbf{T}$, which are now both strain-dependent.

Figure 11 shows how the principal Cauchy stresses depend on the strain, measured by a, when the macroscopic deformation (14) is imposed on the relaxed sample. The left panel shows the average between the principal Cauchy stresses, that is, the eigenvalues of the Cauchy stress tensor $\mathbf{T}$. The right panel shows the anisotropy, which is still defined as $\Delta = (T_{\max} - T_{\min})/T_{\max}$. When a is close to unity, the response is linear, since only the elastomeric thread is in tension. We remark that, even in the linear regime, the anisotropy exhibits a non-monotonic dependence on the strain. This lack of monotonicity is not to be confused with the non-monotonic plot of Figure 9(b), where Δ was studied as a function of the ratio $K_{\text{blue}}/K_{\text{red}}$. Indeed, if we plotted the eigenvalues of the second Piola-Kirchhoff stress tensor $\bar{\mathbf{S}}$, we would have found them to be independent of a in the linear regime. On the contrary, in view of (13), $\mathbf{T}$ depends on a even when $\bar{\mathbf{S}}$ is constant. When $a \gtrsim 2$ the nonlinear thread comes into play, as the plot of $\bar{T}$ evidences. The right panel evidences how the onset of the nonlinear behavior coincides with the inflexion point of Δ which, as usual approaches its maximum allowed value $\Delta = 1$ as a increases.

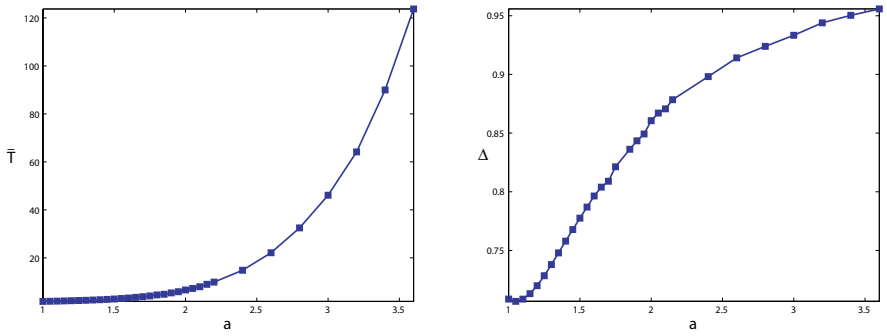

Figure 11: Average stress (left) and anisotropy (right) for a nonlinear tricot textile.

5 Conclusions

In this work we have proposed a new mathematical model and a numerical algorithm for studying the structural properties of textiles. We focused on the estimation of the elastic properties of the textile by minimizing the total energy of the system with respect to the position of the coordinates of the internal nodes. The related multidimensional minimization problem is solved by means of the Nedler-Mead algorithm. As a result we derive a macroscopic strain-energy density whose nonlinear and anisotropic character reflects the topological pattern along which the yarns are knitted. The possibility of knitting together different types of yarns is also included in our analysis, as well as the limiting cases in which the yarns possess very different elastic constants.

We have analyzed both linear and nonlinear models. In the linear case we have proved that the second Piola-Kirchhoff stress tensor $\bar{\mathbf{S}}$ is independent of the macroscopic deformation. Thus, the information on the topology of the textile and the elastic constants of the threads combine to give rise a unique *texture tensor* (defined in (5)) which, combined with (13), allows to compute how the Cauchy stress tensor of the textile depends on the macroscopic deformation.

The nonlinear case appears clearly to be more suited for practical applications. Our proposed nonlinear potential (16) contains several constitutive parameters: the elastic moduli of the threads, a excess length d_1 which models the possibility of knitting a thread in excess, and the length d_2 which characterizes the onset of nonlinearity. However, they are all parameters related to the yarns, and not to the particular topology of the textile. Thus, they can be easily estimated by a suitable fitting procedure in a particular textile - *e.g.*, the tricot textile proposed in our simulations - and then be used to predict the properties of the same yarns when knitted in a different topology.

Possible future developments go along the following directions.

- We have considered planar textiles. However, in real applications, textiles lean on curved substrates. Thus, it will be crucial for practical applications

to generalize the present model to the case in which the knots lie on an assigned curved surface. When this is the case, we expect the curvature tensor to interact with the texture tensor. As a result, further anisotropic properties are expected to manifest. A further development would be obtained by considering the substrate itself as an unknown, by including textile-substrate interactions.

- The knots have been simply modelled by assuming they possess infinite friction. In other words, the yarns are not allowed to slide on each other in their contact points. From the practical point of view, this assumption stands on the thermofixing process which is performed on the fabrics after knitting. Indeed, yarns are almost prevented from sliding after thermofixing is complete. However, a possible generalization of our model would take into account a finite friction coefficient, which would allow sliding when the difference in yarns tension exceeds a critical threshold.

- The microscopic model underlying our macroscopic strain energy allows to identify the knots and the yarns which are more stressed from the mechanical point of view. This is a quite important information for practical purposes, since the yarns which are under greater tension are also more likely to tear. Internal fractures imply a reduction of the elastic constants of the yarns, so that our model is fit to analyze also failures thresholds for the fabrics.

- To possess a numerical algorithm able to capture the macroscopic behavior in terms of the microscopic topology and elastic properties can be a very useful tool in order to anticipate the properties of ideal textiles, without the need of actually weaving real samples. Different knitting topologies are usually classified by simple numerical strings, which serve as input for the weaver machines. It is our aim to develop our numerical algorithm to allow for accepts such numerical strings as inputs for the coding of the knots topology.

Acknowledgement

We are grateful to Alessandro Veneziani, who introduced us to the topic of mathematical and numerical modeling of textile. P.A., A.T. and M.V. have been founded by the project RBIP06HF8S "*Materiali e Tecnologie innnovativi per il Tessile Italiano*", and by the project HOT-FDI "*Hollow and Transparent Fibers Design for Industries*".

References

[1] E. Baesu: *Finite deformation of elasticplastic filamentary networks.* Int. J. Nonlin. Mech. **38** (2003), 14731479.

[2] M.E. Gurtin: *An Introduction to Continuum Mechanics.* Mathematics in Science and Engineering **158**, Academic Press, New York, 1981.

[3] M.J. King, P. Jearanaisilawong, and S. Socrate: *A continuum constitutive model for the mechanical behavior of woven fabrics.* Int. J. Solids Struct. **42** (2005), 3867-3896.

[4] J.C. Lagarias, J.A. Reeds, M.H. Wright, and P.E. Wright: *Convergence properties of the Nelder-Mead simplex method in low dimensions.* SIAM J. Optimiz. **9** (1998), 112-147.

[5] B. Nadler, P. Papadopoulos, and D.J. Steigmann: *Convexity of the strain-energy function in a two-scale model of ideal fabrics.* J. Elasticity **84** (2006), 223-244.

[6] B. Nadler, P. Papadopoulos, and D.J. Steigmann: *Multiscale constitutive modeling and numerical simulation of fabric material.* Int. J. Solids Struct. **43** (2006), 206-221.

[7] B. Nadler and D.J. Steigmann: *A model for frictional slip in woven fabrics.* C. R. Mechanique **331** (2003), 797-804.

[8] A. Quarteroni, R. Sacco, and F. Saleri: *Numerical mathematics.* Texts in Applied Mathematics **37**, Springer-Verlag, Berlin, 2nd Ed., 2007.

[9] Y. Yanagawa, S. Kawabata, and H. Kawai: *Theoretical study on the biaxial tensile properties of warp knitted fabric of single tricot stitch.* J. Text. Mach. Soc. Japan **16** (1970), 88-99.

[10] Y. Yanagawa, S. Kawabata, K. Nakagava, K. Toyama, and H. Kawai: *Experimental study on the biaxial tensile properties of warp knitted fabrics of single tricot stitches.* J. Text. Mach. Soc. Japan **16** (1970), 126-135.

[11] Y. Yanagawa, S. Kawabata, K. Nakagava, K. Toyama, and H. Kawai: *Theoretical study on the biaxial tensile properties of single tricot warp knitted fabric with open lap.* J. Text. Mach. Soc. Japan **16** (1970), 216-228.

[12] Y. Yanagawa, S. Kawabata, and H. Kawai: *Theoretical study on the biaxial tensile properties of plain tricot fabric.* J. Text. Mach. Soc. Japan **17** (1971), 15-25.

MOX Technical Reports, last issues

Dipartimento di Matematica "F. Brioschi",
Politecnico di Milano, Via Bonardi 9 - 20133 Milano (Italy)

31/2009 Paola F. Antonietti, Paolo Biscari, Alaleh Tavakoli, Marco Verani, Maurizio Vianello:
Theoretical study and numerical simulation of textiles

30/2009 Z. C. Xuan, T. Lassila, G. Rozza, A. Quarteroni:
On computing upper and lower bounds on the outputs of linear elasticity problems approximated by the smoothed finite element method

29/2009 P.F. Antonietti, A. Pratelli:
Finite Element Approximation of the Sobolev Constant

28/2009 L. Gaudio, A. Quarteroni:
Spectral Element Discretization of Optimal Control Problems

27/2009 L. Mirabella, F. Nobile, A. Veneziani:
A robust and efficient conservative technique for simulating three-dimensional sedimentary basins dynamics

26/2009 M. Longoni, A.C.I. Malossi, A. Villa:
A robust and efficient conservative technique for simulating three-dimensional sedimentary basins dynamics

25/2009 P.E. Farrell, S. Micheletti, S. Perotto:
An anisotropic Zienkiewicz-Zhu a posteriori error estimator for 3D applications

24/2009 F. Di Maio, P. Secchi, S. Vantini, E. Zio:
Optimized Fuzzy C-Means Clustering and Functional Principal Components for Post-Processing Dynamic Scenarios in the Reliability Analysis of a Nuclear System

23/2009 L. Gerardo Giorda, F. Nobile, C. Vergara:
Analysis and optimization of Robin-Robin partitioned procedures in Fluid-Structure Interaction Problems

22/2009 L. Formaggia, S. Minisini, P. Zunino:
Modeling erosion controlled drug release and transport phenomena in the arterial tissue